

Drift-sensitive non-structural damage to masonry-infilled reinforced concrete frames designed to Eurocode 8

Felice Colangelo

Received: 22 February 2013 / Accepted: 4 August 2013 / Published online: 30 August 2013
© Springer Science+Business Media Dordrecht 2013

Abstract Post-earthquake surveys indicate that losses come from non-structural damage more than from structural damage. Current performance-based design would prevent excessive non-structural damage as well, but the effectiveness of relevant code provisions has not been assessed in depth. This study investigates the drift-sensitive non-structural damage to reinforced concrete frame buildings complying with the European seismic code. Damage to non-structural unreinforced masonry infill walls in contact with the frame is quantified in terms of numerical fragility curves with the same quantities considered in the design: the peak ground acceleration measures the seismic intensity; the peak value of the interstorey drift ratio is the damage index. The methodology for the fragility computation is described in detail. Peculiar is the use of probabilistic parameters of the drift capacity coupled to the fuzziness in the damage state. The drift demand is estimated by member-by-member modelling of typical frame structures and non-linear time–history analyses under spectrum-compatible artificial accelerograms. The kind of the infills and their modelling, the number of storeys, the ground type, and the ductility class are covered. Modelling the infills results to be essential. Any code-compliant verification is on the safe side, but the margin appears to be inconsistent among the frames under consideration. Furthermore, there is one case where occupancy appears to be not ensured despite the code verification is satisfied. The effect of the number of storeys may be misrepresented. The ductility class may be unimportant, however the damage seems to be correlated with the likely strength.

Keywords Eurocode 8 · Fuzzy–random fragility · Infilled frame · Interstorey drift · Non-structural damage

F. Colangelo (✉)

DICEAA Department, University of L'Aquila, Via Giovanni Gronchi 18, 67100 L'Aquila, Italy
e-mail: felice.colangelo@univaq.it

1 Introduction

Post-earthquake surveys indicate that, with the exception of those buildings where severe structural damage or collapse occurs, most economic and social losses result from damage to non-structural components. There are three reasons for this (Taghavi and Miranda 2003). First, the non-structural components represent a large percentage of the total cost of a building, with few exceptions. Second, in comparison with structural damage, non-structural damage starts at a much smaller demand, in terms of both deformation and acceleration. Third, there are a lot of components (electrical, plumbing, mechanical, and conveying systems; doors and windows; contents) all being essential to functionality. A recent confirmation is from the April 6th 2009 L'Aquila, Italy earthquake. Despite it was not so strong (moment magnitude 6.3), some 30,000 people, about half the residents, had to be evacuated, the cause frequently being non-structural damage (Braga et al. 2011). The majority of damage to the San Salvatore hospital was non-structural as well (Augenti and Parisi 2010).

Recent suburban buildings in L'Aquila, as well as in Italy and Southern Europe, have a low- to mid-rise reinforced concrete (RC) frame structure, possibly with RC walls as the lift shaft. Non-structural exterior walls and interior partitions are unreinforced masonry walls made up of clay bricks and cement mortar; they are considerably strong, stiff, and brittle. Most of such buildings comply with force-based design codes merely prescribing strength verification with partial safety factors, if not allowable stresses. However, excessive non-structural damage to new buildings would be prevented by performance-based design and explicit verification of the seismic serviceability limit states, termed "damage limitation" in the European code (CEN 2004b). Eurocode 8 enforces specific measures for the new buildings as above, verbatim (i) with interacting non-engineered masonry infills built after the hardening of the concrete frames; (ii) in contact with, but without structural connection to the frames; and (iii) considered in principle as non-structural elements.

Indeed, despite the many studies to assess the ultimate structural performance ensured by Eurocode provisions (Fardis et al. 2012; Rivera and Petrini 2011; Rozman and Fajfar 2009 among the most recent ones), the studies about the non-structural performance and serviceability are very few (Ricci et al. 2012). The effectiveness of the code provisions to limit non-structural damage still needs validation by numerical simulation, laboratory testing, and post-earthquake survey. All the more so because the current provisions appear to be simplistic, at least because there are a great number and kinds of non-structural components to endanger serviceability, and specific verification of each of them is unfeasible (FEMA 2003).

This study aims to assess the drift-sensitive damage to non-structural masonry infills of RC frame buildings designed following Eurocode 8. The out-of-plane seismic action is not considered; openings in the infills are not covered. The infill damage is quantified in terms of numerical fragility curves. For consistency with the design provisions by Eurocode 8, these curves are computed depending on the peak ground acceleration (PGA) as intensity measure. For the same reason, the peak value of the interstorey drift ratio is assumed to be the damage index. Two kinds of curves are computed. One kind is consistent with the capacity being defined as the threshold drift for the serviceability verification by Eurocode 8. Peculiar to the other kind of curves is the use of proper probabilistic parameters of the drift capacity, coupled with the fuzziness in the non-structural damage state, according to a recent fuzzy-random fragility model (Colangelo 2012, 2013). The drift demand is from member-by-member modelling of frame structures typical of buildings, and non-linear time-history analyses under artificial accelerograms compatible with the design spectrum. The frames are analysed bare in order to derive the former kind of fragility curves, representative of a

fully code-compliant assessment (Eurocode 8 allows one to verify serviceability by analysis of bare frames, as is recalled afterwards). The same frames are analysed infilled as well, in order to derive the fuzzy–random fragility curves representative of realistic non-structural performance. Both kinds of the fragility curves cover four parameters, that is, (i) the kind of the infill: exterior wall and partition; (ii) the number of stories: four and eight; (iii) the ground type: rock-like formation (A ground) and deposit of possibly cohesive soil (D ground); and (iv) the frame ductility class: medium (DCM) and high (DCH).

The features of the building structures and their design, which is important to understand some results, are summarised in Sect. 2. The methodology for the fragility computation is described in detail in Sect. 3. Finally, the fragility curves are presented in Sect. 4.

2 Masonry-infilled RC frame structures

Ordinary residential buildings with a RC frame structure are considered. The construction is regular both in plan and elevation, which also implies uniform arrangement of the masonry infills. Indeed, a prototypal individual planar frame of such buildings is investigated; the accidental torsional effect is not taken into account.

2.1 Configuration

The topology of the analysed frames, 4-storey and 8-storey high, is illustrated in Fig. 1. The tributary areas are 4.0 m wide. The cross-section dimensions resulting from the Eurocode-compliant design (Sect. 2.3) are listed in Table 1 (4-storey frames) and in Table 2 (8-storey frames).

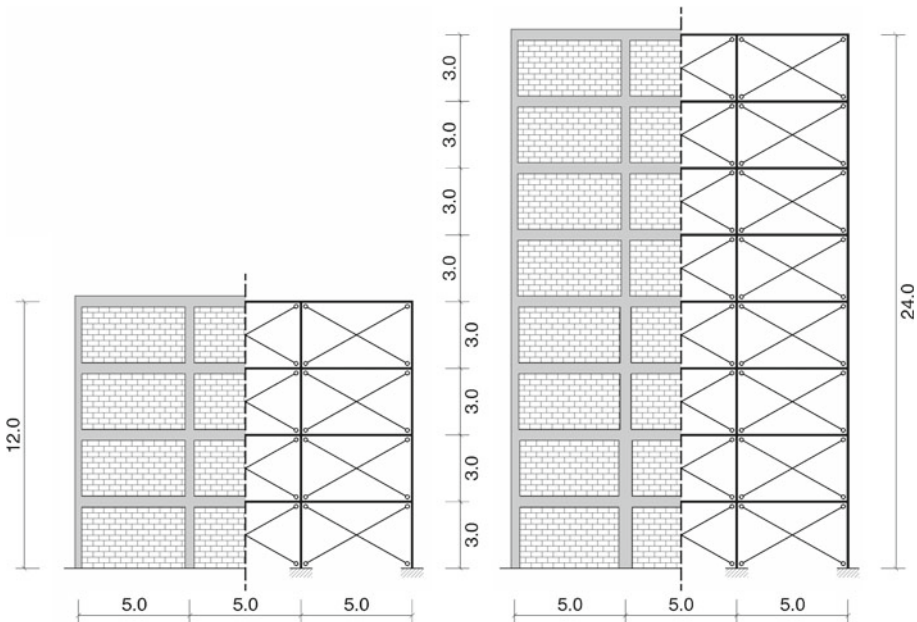


Fig. 1 Configuration and member-by-member model of infilled frames (dimension in m)

Table 1 Dimension of the member cross-sections of 4-storey frames (width times depth in cm)

Storey	DCM frame						DCH frame						
	Type A ground			Type D ground			Type A ground			Type D ground			
	Beam	Column		Beam	Column		Beam	Column		Beam	Column		
	Outer	Inner	Outer	Inner	Outer	Inner		Outer	Inner	Outer	Inner	Outer	Inner
4 and 3	30 × 50	30 × 30	40 × 40	30 × 50	45 × 45	50 × 50	30 × 50	30 × 30	40 × 40	30 × 50	45 × 45	50 × 50	
2 and 1	30 × 50	30 × 30	40 × 40	30 × 50	50 × 50	55 × 55	30 × 50	35 × 35	45 × 45	30 × 50	50 × 50	55 × 55	

Table 2 Dimension of the member cross-sections of 8-storey frames (width times depth in cm)

Storey	DCM frame						DCH frame						
	Type A ground			Type D ground			Type A ground			Type D ground			
	Beam	Column		Beam	Column		Beam	Column		Beam	Column		
	Outer	Inner	Outer	Inner	Outer	Inner		Outer	Inner	Outer	Inner	Outer	Inner
8 and 7	30 × 50	30 × 30	40 × 40	30 × 50	45 × 45	50 × 50	30 × 50	30 × 30	40 × 40	30 × 50	45 × 45	50 × 50	
6 and 5	30 × 50	30 × 30	45 × 45	30 × 60	55 × 55	60 × 60	30 × 50	35 × 35	45 × 45	30 × 60	55 × 55	60 × 60	
4 and 3	30 × 60	35 × 35	50 × 50	40 × 60	60 × 60	65 × 65	30 × 60	40 × 40	50 × 50	40 × 60	60 × 60	65 × 65	
2 and 1	30 × 60	40 × 40	55 × 55	40 × 60	60 × 60	65 × 65	30 × 60	45 × 45	55 × 55	40 × 60	60 × 60	65 × 65	

As mentioned above, all frames are analysed both bare and uniformly infilled by non-structural unreinforced masonry of perforated bricks and cement mortar. Two kinds of infill walls with the same basic mechanical properties are considered. One infill, termed “weak”, is 8 cm thick and represents an interior, single-wythe partition. The other infill, termed “strong”, may correspond to an exterior wall or a wall separating two apartments. It consists of two unconnected weak infills with in-between insulant, as usual in practice (Braga et al. 2011). Clearly, both strength and stiffness of the strong infill as a whole double, while its drift capacity may be considered to be the same as that of the weak infill.

2.2 Behaviour model

The frame members are modelled one-to-one as linearly elastic beam elements provided with flexural hysteretic springs at their ends. Any different failure, those of the beam-column joints as well, are not considered as deemed to be prevented by design. The stiffness of the beam element is equal to one-half of the stiffness corresponding to the gross dimension of the concrete cross-section, in order to account for cracking (CEN 2004b). The terminal springs are elastic–plastic with hardening and follow the cyclic model by Takeda et al. (1970) as simplified by Otani (1974) and by Litton (1975). In brief, the post-yielding unloading stiffness decreases depending on the plastic rotation. The reloading branch heads for the previous extreme reversal point on the first-loading curve, in the same loading direction. The strength deterioration and variation in the yielding moment with variation in the axial force are both neglected. A sample loading path of a RC member as a whole is shown in Fig. 2a.

Each infill wall is idealised as a pair of equivalent diagonal struts connecting the frame joints and reacting in compression only, that is, one at a time under horizontal loading (Fig. 1). The cyclic model “no. 2” by Panagiotakos and Fardis (1997) is adopted. This

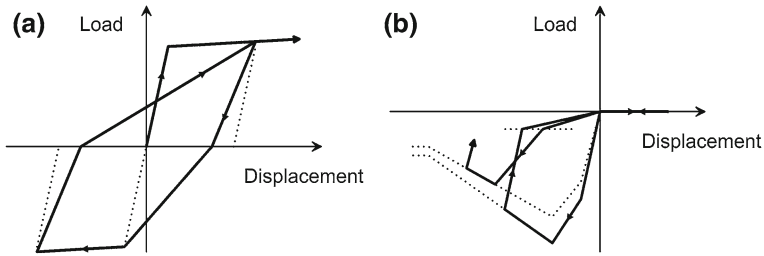


Fig. 2 Behaviour model of **a** RC member and **b** strut equivalent to infill wall

is based on a multi-linear envelope curve defined by the first cracking, the peak strength, and failure, beyond which some residual strength remains. The first-cracking load and the initial (uncracked) stiffness derive from the shear strength and the shear modulus of the infill masonry; the peak strength and the (cracked) stiffness secant from the first cracking to the peak strength derive from the compressive strength and the Young modulus, with the height of the strut cross-section taken equal to one-eighth of the strut length. Pinching, the strength decrease in reloading, and deterioration of the envelope curve appear under cycling. A sample loading path of a single strut is illustrated in Fig. 2b.

Such a phenomenological model can simulate the seismic time-history response of infilled frames, and represent their damage states as well, conditional on a proper calibration (Colangelo 2003). Such a calibration was carried out on the basis of pseudo-dynamic (PD) test results on one-storey one-bay infilled-frame specimens (Colangelo 2005). The numerical parameters in detail and related discussion can be found elsewhere (Colangelo 2003). The underlying material properties are mentioned in Sect. 2.3.

2.3 Design

The frames under consideration are designed with the load and resistance (partial) safety factor method (CEN 2002a) and linear structural analysis. The C25/30 concrete class is assumed; the mean value of the cylinder compressive strength is equal to 33 MPa (CEN 2004a). The characteristic and mean values of the yield strength of reinforcing steel are 450 and 530 MPa, respectively. The strengths and the safety factors of concrete and steel in the fundamental load situation are used in the seismic ultimate situation as well, assuming that the strength deterioration due to seismic cycling (CEN 2004b) balances the factor decrease allowed in the accidental situation (CEN 2004a). With regard to the mean values of the infill masonry properties, the shear and Young moduli are equal to 1.1 and 2.0 GPa, respectively; the shear and compressive strengths are equal to 1.0 and 5.0 MPa, respectively. Such values are consistent with a number of vertical, horizontal, and diagonal compression tests on small-sized walls made up of differently perforated bricks (Colangelo 2005).

The characteristic value of the self-weight load on the beams is equal to 32 kN/m on the residential floors, and to 24 kN/m on the roof. The characteristic value of the imposed load amounts to 2 kN/m² on every storey (CEN 2002b). The seismic action is represented by the type 1 linear response spectrum (CEN 2004b) with the design PGA on the type A ground assumed to be equal to 0.25 g, to be multiplied by the soil factor equal to 1.35 for the type D ground. Note that the soil factor for the type E ground is even greater, but the constant-acceleration branch of the type 1 spectrum is much wider for the type D ground (CEN 2004b), thus this ground type is selected for the study. The self-weight load G , the imposed load Q , and the seismic action A_E are combined as usual in the ultimate situation:

$$\begin{cases} \gamma_G G_k'' + \gamma_Q Q_k \\ G_k'' + \psi_2 Q_k'' + A_{Ek} \end{cases} \quad (1)$$

where the factor values depend on the loading effect, which may be unfavourable or not (CEN 2002a). The seismic effect results from linear multi-modal response-spectrum analysis with the behaviour factor q being equal to 3.90 and 5.85 for the DCM and DCH ductility classes, respectively; present on the frames is the mass associated with the load reduced as follows (CEN 2004b):

$$G_k'' + \varphi \psi_2 Q_k \quad (2)$$

Provided that any undesired failure mode is prevented, five provisions govern the frame design (CEN 2004b). First, obviously, there is the flexural resistance condition. Second, aiming for a suitable plastic mechanism, flexural overstrength is required from the columns with respect to the beams framing into each joint:

$$r = \frac{\sum M_{Rc}}{\sum M_{Rb}} \geq 1.30 \quad (3)$$

M_{Rb} and M_{Rc} , respectively are the resisting bending moments of the beams and those of the columns (their minimum values depending on the axial force in the seismic design situation), summed in Eq. 3 according to the joint equilibrium. Third, the local ductility condition governs detailing; it also limits the normalised axial force ν in the columns in the seismic design situation:

$$\nu \leq \begin{cases} 0.65 \text{ DCM class} \\ 0.55 \text{ DCH class} \end{cases} \quad (4)$$

Fourth, for the purpose of avoiding second order effects, it should result in all storeys:

$$\theta = \frac{P}{V} \cdot \frac{d}{h} \leq 0.10 \quad (5)$$

P is the total gravity load on the storey under consideration in the seismic design situation; V is the storey shear; d/h is the interstorey drift ratio. Strictly speaking, such a limitation is recommended, not mandatory. However, this study complies with Eq. 5 believing that practising engineers would do in order to bypass non-linear analysis as well as any effect amplification depending on θ . Finally, as regards serviceability, the damage limitation requirement is deemed to be satisfied by limiting the interstorey drift ratio. For ordinary buildings with non-structural elements of brittle materials attached to the structure, which is the case, it holds:

$$\Delta = \frac{0.5d}{h} \leq 0.5 \% \quad (6)$$

Note that 0.5 in Eq. 6 stands for the reduction factor specific to ordinary buildings (importance class II) to take into account the lower return period with respect to the seismic action in the ultimate situation, as in Eq. 5. According to Fardis et al. (2012), the slenderness limit by Eurocode 2 (CEN 2004a) may be more demanding than Eq. 6, and lead to larger cross-section of the RC members. This is not considered in this study. Also note that infills do not play any role in all of these provisions, because Eurocode 8 compels one to model the infills only in the case of RC DCH systems with severe irregularities in the infill arrangement (CEN 2004b). Incidentally, the earlier Eurocode 8 part 1–3 dated November 1994 prescribed to consider the spectrum ordinate at the average between the period of oscillation of the bare frame and that of the infilled frame, which does not appear in the present Eurocode 8 anymore.

Table 3 Design quantities of 4-storey frames

Quantity	DCM frame						DCH frame					
	Type A ground			Type D ground			Type A ground			Type D ground		
	Bare	Infilled		Bare	Infilled		Bare	Infilled		Bare	Infilled	
		Weak	Strong		Weak	Strong		Weak	Strong		Weak	Strong
T_1 (s)	0.814	0.298	0.226	0.577	0.270	0.206	0.730	0.289	0.219	0.577	0.270	0.206
T_2 (s)	0.268	0.105	0.084	0.179	0.092	0.072	0.249	0.102	0.080	0.179	0.092	0.072
T_3 (s)	0.162	0.069	0.060	0.098	0.057	0.048	0.150	0.065	0.057	0.098	0.057	0.048
V_{base} (%)	6.8	13.7	13.4	17.3	18.3	18.4	4.9	9.1	9.0	11.6	12.3	12.3
Δ_{max} (%)	0.37	–	–	0.50	–	–	0.31	–	–	0.50	–	–
θ_{max}	0.09	–	–	0.05	–	–	0.10	–	–	0.07	–	–
r_{min}	1.32	–	–	2.08	–	–	1.35	–	–	2.44	–	–
ν_{max}	0.42	–	–	0.21	–	–	0.33	–	–	0.21	–	–

Table 4 Design quantities of 8-storey frames

Quantity	DCM frame						DCH frame					
	Type A ground			Type D ground			Type A ground			Type D ground		
	Bare	Infilled		Bare	Infilled		Bare	Infilled		Bare	Infilled	
		Weak	Strong		Weak	Strong		Weak	Strong		Weak	Strong
T_1 (s)	1.228	0.583	0.469	0.867	0.505	0.406	1.177	0.567	0.453	0.867	0.505	0.406
T_2 (s)	0.449	0.201	0.163	0.313	0.171	0.137	0.435	0.195	0.157	0.313	0.171	0.137
T_3 (s)	0.260	0.115	0.092	0.177	0.099	0.079	0.252	0.112	0.089	0.177	0.099	0.079
V_{base} (%)	4.4	8.8	10.6	15.2	17.1	17.1	3.9	6.1	7.4	10.2	11.5	11.5
Δ_{max} (%)	0.28	–	–	0.50	–	–	0.26	–	–	0.50	–	–
θ_{max}	0.10	–	–	0.06	–	–	0.10	–	–	0.09	–	–
r_{min}	1.34	–	–	1.86	–	–	1.40	–	–	2.50	–	–
ν_{max}	0.45	–	–	0.30	–	–	0.44	–	–	0.30	–	–

The outcome of the design as above is summarised in Table 3 (4-storey frames) and in Table 4 (8-storey frames). It is repeated that this is important to understand some results of this study. The tables start with the first periods of oscillation with prevailing horizontal displacement, then there is the design base shear as percent of the weight in the seismic situation (Eq. 1). For the sake of comparison, such quantities are listed for the bare and infilled frames as well. In the modal analysis, consistent with the stiffness of RC members being halved to account for cracking, the stiffness of the infills is assumed to be the stiffness secant from the origin to the peak strength, which amounts to 35 % of the shear stiffness of the uncracked walls. Even so, in comparison with the bare frame the periods decrease to a great extent, whatever the infill kind may be. The base shears almost double on the type A ground. However, perhaps unexpectedly, the base shears remain similar on the type D ground, due to the wide constant-acceleration branch of relevant response spectrum.

The greater spectral acceleration on the type D ground, and its spanning a wider range of periods as well, cause the cross-section dimensions to be increased with respect to the type A

ground, as seen in Tables 1 and 2. In actual fact, the requirements about deformation govern the dimensions. The condition to avoid second order effects (Eq. 5) governs on the type A ground, whereas the damage limitation verification (Eq. 6) does on the type D ground (see Δ and θ maxima among all storeys in Tables 3 and 4).

The effect of the ductility class may be unexpected and deserves attention. Since the inelastic interstorey displacement d in the seismic situation is assumed to be independent of the ductility class, Eq. 6 is as well. The cross-section dimensions cannot be reduced where Eq. 6 governs, that is, on the type D ground, despite the design strength of a DCH frame is less than that of a DCM frame. On the other hand, Eq. 5 becomes more demanding for a DCH frame. As the storey shear V decreases following the increased behaviour factor, θ increases. The cross-section dimensions must be increased where Eq. 5 governs, that is, on the type A ground, and this is fulfilled by increasing the column dimensions (compare the DCM dimensions with the DCH dimensions in Tables 1 and 2). Therefore, the DCH class does not yield saving the member dimensions.

In general, the reinforcement ratio for flexural resistance of the beams is greater than the minimum required by the local ductility condition; the same ratio in the columns would be less than their minimum, which must be placed. However, the minimum reinforcement in the columns is close to that strictly necessary to the overstrength condition (Eq. 3) on the type A ground; unfortunately, the minimum reinforcement is excessive for the overstrength condition on the type D ground (see r minimum among all joints in Tables 3 and 4). The margin of the overstrength condition is the greatest for both the DCH frames on the type D ground. Compared with the DCM frames on the same ground, the columns are similarly strong (because of the equal dimensions to satisfy Eq. 6, as explained above, and the necessity to place the minimum reinforcement) but the beams are weaker following the increase in the behaviour factor.

The additional condition on the normalised axial force in the columns (Eq. 4) is satisfied by a wide margin (see ν maximum among all columns and ultimate situations in Tables 3 and 4).

The likely strength of the frames, bare and with weak and strong infills as well, is appraised by the pushover curves resulting from the mean values of the material strength (Fig. 3). The base shear normalised by the weight in the seismic situation (Eq. 1) is illustrated depending on the roof displacement normalised by the frame height. The lateral forces are proportional

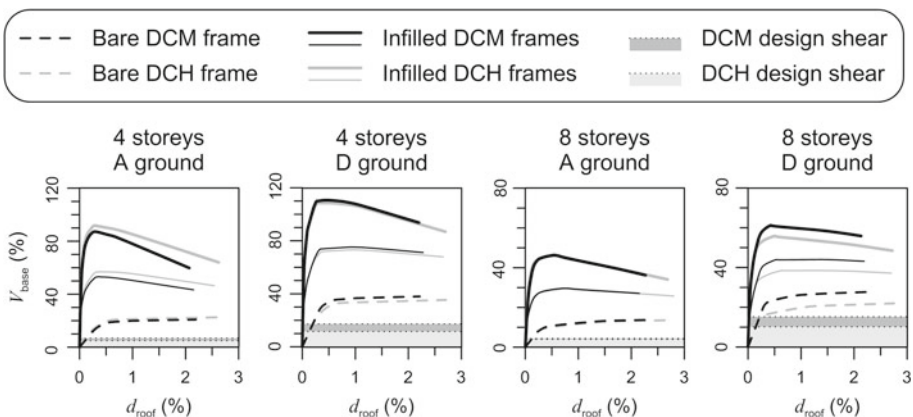


Fig. 3 Pushover curves of bare and infilled frames

to the storey masses and follow the first mode of oscillation. As expected considering the design spectra, each bare frame on the type D ground is stronger than the corresponding bare frame on the type A ground. The bare DCH frames on the type A ground are not weaker than the bare DCM frames on the same ground; this results from a lesser strength of the beams (because of the increased behaviour factor) but a greater strength of the columns (because of the increased dimensions to satisfy Eq. 5, and the necessity to place the minimum reinforcement). The bare DCH frames on the type D ground are to some extent weaker than the bare DCM frames on the same ground; this results from a lesser strength of the beams and a similar strength of the columns (because of the equal dimensions to satisfy Eq. 6, with the minimum reinforcement). Obviously, the strength increase caused by the infills remains almost the same, irrespective of the ground type and the ductility class. Note that the peak strength of the 4-storey frames with strong infills becomes as high as the seismic weight and more. On the other hand, the strength deterioration associated with cyclic loading (Fig. 2b) is greater than that seen in Fig. 3. For the sake of comparison, the design base shears of the bare frames, already seen in Tables 3 and 4, are also illustrated as shaded thresholds in Fig. 3.

3 Methodology for fragility computation

Three key tasks are involved, that is: (i) estimation of demand, (ii) estimation of capacity, and (iii) estimation of the fragility associated with such a demand and capacity. This is presented in some detail in the following subsections.

3.1 Estimation of drift demand

The demand is estimated in terms of probabilistic parameters of the peak interstorey drift ratio. This comes from non-linear time-history analyses with the behaviour model said in Sect. 2.2 subjected to a number of code-compatible artificial accelerograms, and statistical inference. The material properties are assumed to be deterministic, thus randomness is due to the ground motion only. Since the fragility curve is of concern, the generation of artificial accelerograms, time-history analyses, and statistical inference are repeated at each and every PGA value from 0.05 to 0.95 g by step 0.05 g.

3.1.1 Artificial accelerograms

Statistically independent, artificial acceleration time histories are generated so as to match the 5% damped linear response spectrum in the horizontal direction by Eurocode 8. Two families of accelerograms are generated, each proper to the type 1 spectrum for either the type A or the type D ground. Among the many methods to simulate the seismic ground motion (see Ólafsson and Sigbjörnsson 2011 for a recent, concise review from origins) the long-established method by Shinozuka and Deodatis (1991) is adopted in this study. The ground acceleration is idealised as a truncated cosine series with stationary frequency content and intensity made time-dependent by a deterministic modulating function:

$$a_g(t) = \sum_i \sqrt{2G(\omega_i) \Delta\omega} \cos(i\Delta\omega t + \phi_i) \cdot f(t) \quad (7)$$

$G(\omega)$ is the one-sided power spectral density function (PSDF). $\Delta\omega$ is a discrete increase to circular frequency. ϕ_i 's are random phase angles independent of each other and uniformly distributed between 0 and 2π . $f(t)$ is the modulating function. The PSDF can be formulated

depending on the linear response spectrum and the peak factor relevant to a given response duration and exceedance probability, estimated independently of the PSDF moments for convenience (Vanmarcke 1976). In order to make the computed response spectrum fit the target response spectrum prescribed by Eurocode 8, the PSDF is adjusted specifically to each accelerogram by comparing its own response spectrum with the target one. Such an adjustment is iterative, that is, each accelerogram is expanded by Eq. 7 whenever its PSDF is adjusted.

Further assumptions are as follows. The spectrum ordinates are intended as 50% percentiles. The type 1 spectrum is assumed at every PGA, despite the type 2 spectrum would be better for low magnitude (CEN 2004b). The modulating function is shaped as the trapezoid shown in Fig. 4a. With regard to time t_s , it is well-known that the earthquake duration correlates with magnitude, distance, and ground type, at least. However, the duration seems to be statistically insignificant to the displacement ductility demand (it is recalled that herein the drift is the damage index), whichever the period of oscillation and stiffness deterioration are (Iervolino et al. 2006). Nonetheless, the strength deterioration typical of masonry correlates with duration, as one would expect (Bommer et al. 2004). Since the infill model incorporates the strength deterioration (Fig. 2b), duration is made dependent on PGA. Following the earlier Eurocode 8 part 1–1 dated May 1994, the stationary duration would increase with the effective PGA; this is introduced depending on the design PGA as shown in Fig. 4b.

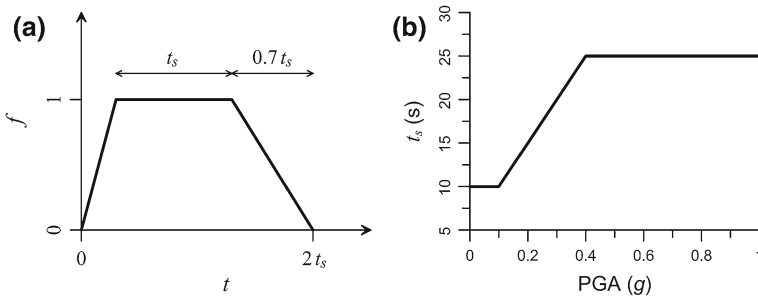


Fig. 4 a Modulating function and b stationary duration of artificial accelerograms

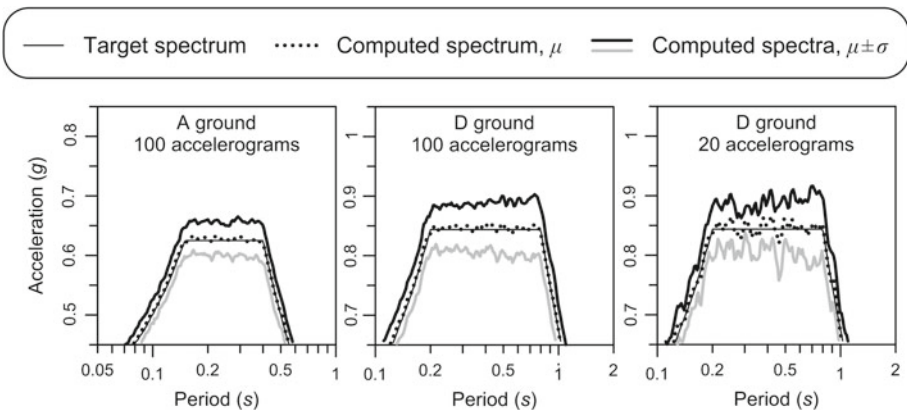


Fig. 5 Target spectra versus statistics on computed spectra

The computer program SIMQKE-1 (Vanmarcke et al. 1976) was modified and made fully consistent with formulation above. The random phase angles in Eq. 7 follow the 64-bit arithmetic algorithm recommended by Press et al. (2007). Shown in Fig. 5 are the Eurocode 8 spectra together with statistics on the response to the artificial accelerograms, namely the mean μ and the mean plus and minus one standard deviation σ . Clearly, 100 accelerograms yield a very good agreement between the target and mean spectra, and stable statistics of the spectra ordinates as well, which do not appear with the use of 20 accelerograms or so.

3.1.2 Non-linear time-history analysis

A modified version of the computer program ANSR-I (Mondkar and Powell 1975a,b) is used to analyse the frames. Integration is carried out by the Newmark method with numerical damping prevented in the linear stage. Viscous damping is defined as being proportional to the global mass and tangent stiffness matrices, so that the viscous damping ratio is equal to 5% in the first and third (linear) mode of oscillation with prevailing horizontal displacement. The mean values of the material strength (concrete, steel, and masonry) are used. Consistent with the frame design (Eq. 5), second order effects are omitted.

3.1.3 Probabilistic distributions

The probabilistic parameters of the demand are inferred from the drift samples at each PGA value by the method of moments (Soong 2004). For instance, the mean value, standard deviation, and coefficient of variation (CoV, labelled δ_s) of the drift demand to some storeys are shown in Fig. 6. Two typical results may be noted incidentally. First, the demands to the storeys of the bare frame (left-hand graphs) are much more similar to each other than in the case of the infilled frame (right-hand graphs), where drift and damage tend to concentrate in the lower storeys. Second, the infills cause the drift to decrease to a noticeable extent even in the lower storeys, until the infills retain their stiffness, that is, where PGA is relatively low (compare the graphs of the second storey).

In a few cases, the time-history analyses and statistical inference were carried out with up to 200 accelerograms. The mean values and CoVs become reasonably stable at a sample size equal to 100 (for instance, see Fig. 7), thus such a size is assumed hereafter. It also results that the demand distribution may be assumed to be lognormal. In actual fact, the coefficients of determination (Draper and Smith 1998) of the regression curves of the drift values on lognormal random variables are greater than 80%, and greater than 90% in most cases.

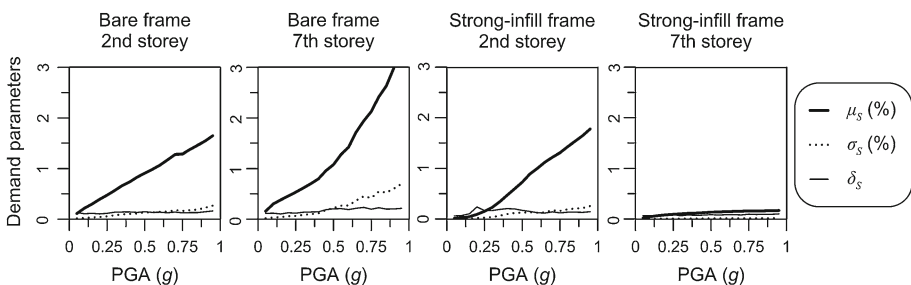


Fig. 6 Probabilistic parameters of drift demand (8-storey DCM frames on type A ground)

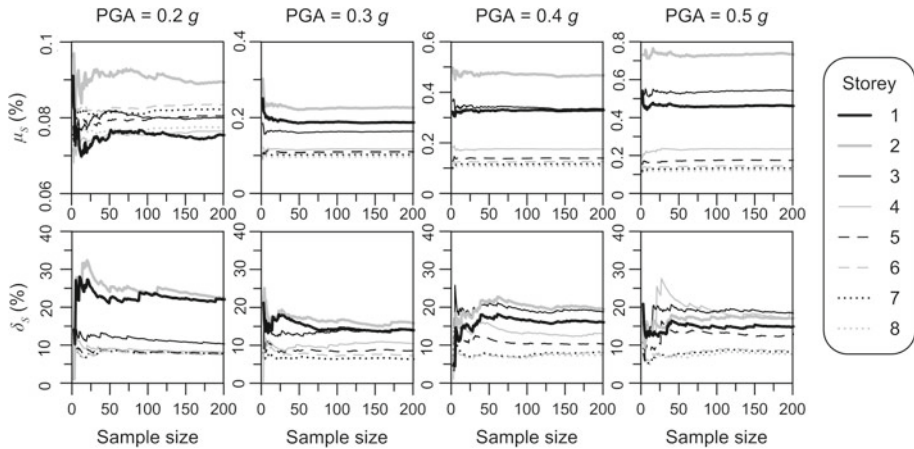


Fig. 7 Sensitivity to sample size (8-storey DCM frame with strong infills on type A ground)

3.2 Estimation of drift capacity

Establishing a reliable association of the peak interstorey drift ratio with degrees of damage and performance levels remains one of the most important unresolved issues in performance-based design (Ghobarah 2004). One reason is that reducing the cause of seismic damage to the maximum deformation, as it suits engineering practice, is a clear oversimplification, all the more so with regard to non-structural elements. The proposals by codes and researchers, in terms of threshold values and probabilistic distributions as well, are reviewed in the following subsections in order to provide the methodology with the most robust basis.

3.2.1 Thresholds in the codes

As mentioned in Sect. 2.3, Eurocode 8 (CEN 2004b) prescribes a drift limit in order to ensure protection against unacceptable damage to ordinary buildings, that is, the damage limitation limit state. With regard to brittle non-structural elements attached to the structure, this limit is 0.5% (Eq. 6), to be applied conventionally to frames analysed bare. It is explicitly stated that this may not suffice to maintain operation for civil protection, therefore such a limit corresponds to some degree of non-structural damage.

The FEMA (2000) prestandard is quite detailed. Four non-structural performance levels are classified concerning both serviceability (“operation” and “immediate occupancy”) and ultimate conditions (“life safety” and “hazards reduced”). The limit for exterior walls differs from the limit for heavy partitions (light partitions may be drywall partitions with studs, for instance) at both the occupancy and life safety performance level. At the occupancy level, there is the limit 0.5% (the same as Eurocode 8) for heavy partitions, while 1% appears for exterior walls; at the life safety level, such limits double.

The Italian code (DM 14/1/2008 2008) also prescribes the limit 0.5% to ensure occupancy; 0.5% times 2/3 is prescribed to ensure operation for civil protection. Moreover, with regard to existing buildings, the commentary (CM 617 2009) declares that both limits are to be reduced if the analysis model includes the infills. In such a case, the limits become the same as for the masonry buildings, which are equal to 0.3 and 0.2% to ensure occupancy and operation, respectively. Consistent with the Italian commentary, this picture may be completed with the

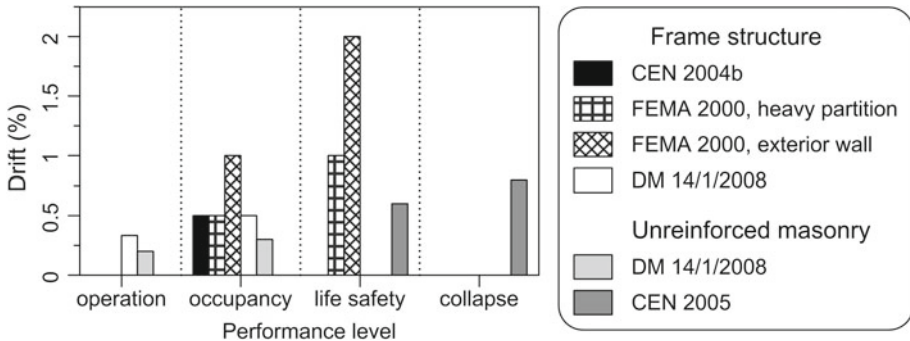


Fig. 8 Drift limits according to codes (performance levels by different codes are assumed to coincide, irrespective of their names)

Eurocode 8 limits for existing masonry buildings in the ultimate limit states (CEN 2005). The most pertinent to infills would be the limits for secondary walls under prevailing shear, which are equal to 0.6 and 0.8 % in the “significant damage” and “near collapse” limit state, respectively.

All the mentioned limits appear to reasonably agree with each other (Fig. 8). Most importantly, the limit for masonry clearly is less than the limit for the bare frame. Estimating the drift demand with the infills being included in the building model, and comparing such a demand with the drift capacity of non-structural masonry, is rational and realistic. Verification with a bare frame model and the drift capacity increased with respect to that of the infills, is fictitious and questionable, but fully code-compliant. In this study, so-termed code-compliant fragility curves are calculated with the drift demand from the bare frame analysis and the limit 0.5 % as threshold against loss of occupancy.

3.2.2 Thresholds in the literature

Deterministic thresholds are proposed in association with the severity of damage to non-structural masonry infills, rather than the performance levels in the codes (Calvi 1999; FEMA 2003; Ghobarah 2004; Masi 2003; Mosalam et al. 1997; Rossetto and Elnashai 2003). The damage degrees are distinguished on the basis of (i) the description of physical damage in terms of cracking, crushing, etc. and (ii) the feasibility of repair. The lowest degree may be said to correspond to the onset of cracking, that is, cosmetic impairment or little more; the second degree implies some loss of serviceability because it requires more than aesthetic repair (Özcebe et al. 2012; Taghavi and Miranda 2003). Such definitions respectively suggest the operation and occupancy performance level, but any correspondence is not obvious. The damage degrees in the scales by different researchers may vary in number, while similar labels, e.g. moderate damage, may refer to different degrees of actual damage (Hill and Rossetto 2008).

Consequently, the drift limits in the literature are illustrated depending on the damage severity, and assuming the damage states to be equally spaced between no damage and failure, irrespective of the number of the damage degrees (Fig. 9). The limits for the bare frames are illustrated together with the Eurocode 8 limit to ensure occupancy (Fig. 9a). Such limit corresponds to intermediate damage on average over the references, which is reasonable. Unfortunately, three references only deal with the infilled frames. Rossetto and Elnashai (2003) suggest limits specific to European-type RC buildings on the basis of post-earthquake

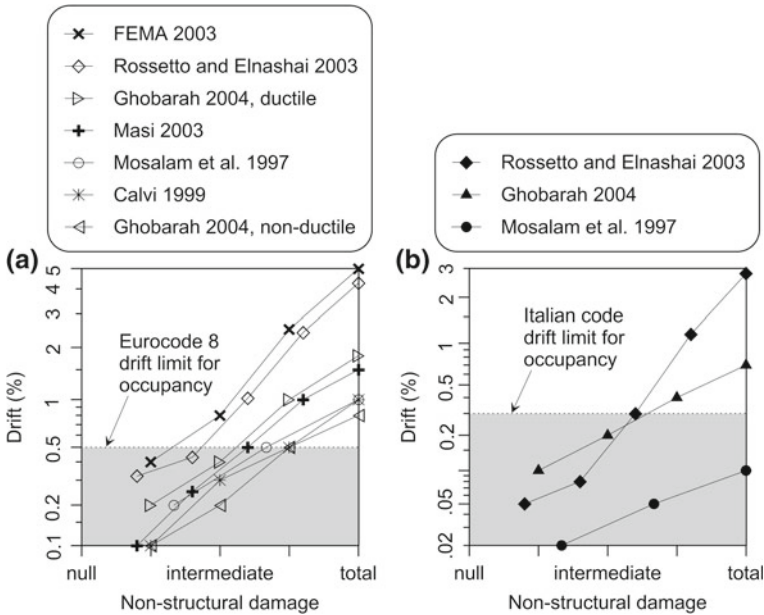


Fig. 9 Drift limits according to researchers for **a** bare frames and **b** infilled frames

surveys providing the damage description, plus laboratory test results providing both the damage description and related drift. Ghobarah (2004) mentions test results and numerical analyses, with the drift of the infilled frames said to be about half the drift of the bare frames. Mosalam et al. (1997) invoke engineering judgement and PD and shaking-table test results on low-rise frames, to assume the limits for the infilled frames to be as small as one-tenth of the limits for the bare frames. This decision seems to be extreme, even in comparison with the limit for masonry by the Italian code, which reasonably corresponds to intermediate damage according to the other researchers (Fig. 9b).

3.2.3 Probabilistic distributions

The probabilistic distributions of the drift at certain degrees of damage to non-structural masonry infills are few. As far as the author knows, three references only can be considered.

On the basis of the PD tests used to calibrate the behaviour model of the infilled frames (Sect. 2.2), the author distinguishes four damage states (Table 5, top part). As soon as each damage state was deemed to be attained by each specimen under PD testing, the peak drift was registered. The peak drift at the same instant is also taken from any time history simulated by the behaviour model, which obviously does not fit exactly the PD time history. The drift from PD testing or simulation yields different parameters of the distributions, which may be assumed to be lognormal (Colangelo and Stornelli 2008), like the demand distributions. The CoV from simulation is greater than that from PD testing, as it must be because modelling introduces additional uncertainty (Colangelo 2013). Moreover, there is cognitive uncertainty. Any definition of limit state in terms of physical damage and feasibility of repair, for instance as in Table 5, inherently is imprecise, qualitative, and open to individual judgment. The boundary between different states, e.g. acceptable versus unacceptable damage, usually is not clear; indeed, a ductile behaviour implies gradual transition from a damage state to

Table 5 Probabilistic parameters of drift capacity according to researchers

Reference	State	Damage description and/or performance level	Randomness alone		Randomness and fuzziness		
			μ_R (%)	δ_R (%)	μ_R (%)	δ_R (%)	γ
Colangelo (2013)	1st	Onset of cracking in the bricks, associated with the first noticeable reduction of stiffness	0.029	59.9	0.038	40.3	0.432
	2nd	Moderate cracks before attaining the maximum strength (i.e. base shear)	0.350	96.5	0.493	53.5	0.450
	3rd	Extensive cracks with tensile splitting and falling of the outer layer of a few bricks; repairable damage	0.849	62.7	1.070	46.3	0.439
	4th	So many broken bricks that repair is unreasonable; reconstruction needed	1.618	23.7	1.784	12.8	0.243
Gu and Lu (2005)	1st	Minor cracking and falling of plaster; only local repair needed with function maintained; maximum strength	0.254	82.8	–	–	–
	2nd	Continual diagonal cracking and flaking; repairable damage; 30% reduction of the maximum strength	0.541	74.8	–	–	–
	3rd	Loss of wall integrity; 70% reduction of the maximum strength	0.801 ^a	43.1 ^a	–	–	–
Özcebe et al. (2012)	1st	Negligible cracks; maximum strength (i.e. base shear)	0.079	23.5	–	–	–
	2nd	Appreciable damage; maximum stress in the infill	0.102	23.1	–	–	–
	3rd	Ultimate strain in the infill	0.227	37.1	–	–	–

^a Normal distribution a little better than lognormal distribution

the next one. This is cognitive uncertainty, or fuzziness, to be considered beside stochastic uncertainty due to the randomness of earthquakes, material properties, etc. To this end, an analytical fuzzy–random model has been proposed (Colangelo 2012) and fully characterised in probabilistic terms, including the parameter estimation (Colangelo 2013). This model is consistent with the time-invariant first-order second-moment reliability method. Demand and capacity are assumed to be lognormal random variables independent of each other. Peculiar is the membership function, proposed to be a piecewise second-degree polynomial, to express the degree of membership in a damage state. Fragility is the probability of occurrence of a random event with fuzzy description (the damage state), measured in the probabilistic framework as the expected value of the membership function (Zadeh 1968). Samples of the degree of membership in each damage state may be obtained by pairwise comparisons (Saaty 2008), then the proposed model allows one to estimate the fuzziness parameter and the probabilistic parameters of the drift capacity in a coupled fashion (Colangelo 2013).

Such parameter values are in Table 5 (top part). The mean value and CoV of the drift from the behaviour model are listed in both the cases of the fuzziness being neglected or

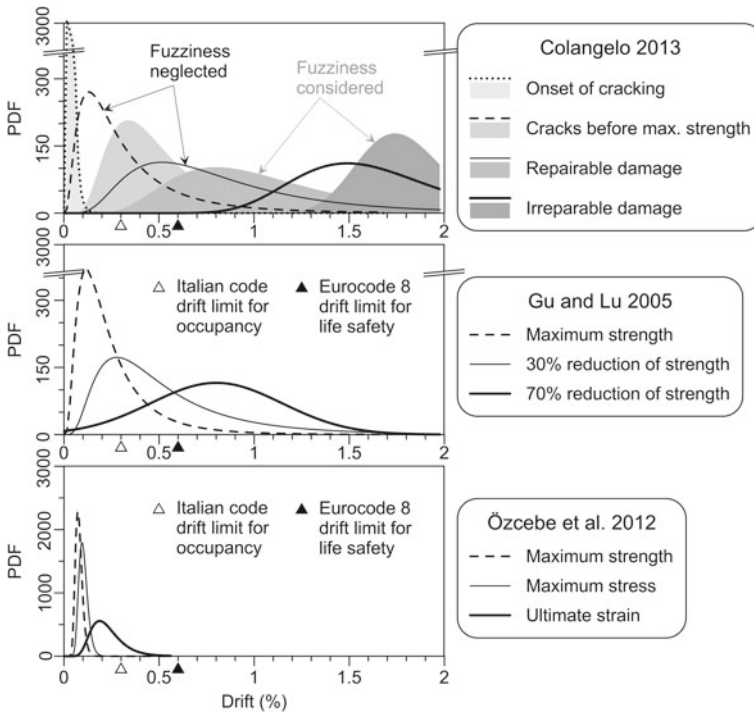


Fig. 10 PDFs of drift according to researchers

considered. In the latter case (final columns), the mean values are greater, the CoVs are lesser. In fact, dispersion of the drift values is attributed partly to randomness and partly to fuzziness, rather than entirely to randomness (Colangelo 2013). The mean value at the first cracking is quite small, consistent with PD samples ranging from 0.019 to 0.029 % (Colangelo 2005). Measurements as small as 0.02–0.04 % have been confirmed recently (Zovkic et al. 2013) and may support the low threshold by Mosalam et al. (1997) mentioned in Sect. 3.2.2, but damage as slight as the first cracking should be of concern, which is not the case of occupancy. In Table 5, γ denotes the fuzziness parameter ranging from 0 to 1 (Colangelo 2012). It appears to be nearly intermediate and constant except for the final state, where the fuzziness results to be lesser. As far as the author knows, this is the only estimation of probabilistic parameters of the drift capacity within a fuzzy–random approach to the damage assessment. Comparison is possible only with cases of randomness alone.

Gu and Lu (2005) select and process a group of unreinforced brick masonry walls from among some 140 masonry specimens under in-plane lateral loading. They define three performance levels termed “functional” (74 samples), “damage control” (20 samples), and “collapse” (20 samples), each associated with the damage description, location in the load-displacement curve, and probabilistic parameters of the drift (Table 5, middle part).

Finally, Özcebe et al. (2012) carry out adaptive pushover analyses of 20 poorly-designed European-type infilled RC frame structures. They define three damage degrees and their association with results from the pushover analysis. The drift values calculated for every case study are reported in the original paper, thus the probabilistic parameters can be inferred. On the assumption that the distributions are lognormal, the method of moments (Soong 2004) yields the parameter values in Table 5 (bottom part).

For ease of comparison, the probability density functions (PDFs) are illustrated in Fig. 10; the shaded PDFs are those from coupled randomness and fuzziness, thus they do not have any counterpart. The damage descriptions in Table 5 suggest that the damage states no. 2–4 by Colangelo (2013) may correspond to the damage states by Gu and Lu (2005). In fact, the only clear inconsistency is which state the maximum strength would be attained at. The PDFs in the final state differ to some extent, as regards the mean value especially, however the other couples of PDFs match reasonably well (top and middle graphs in Fig. 10). On the contrary, the PDFs by Özcebe et al. (2012) from modelling rather than testing (bottom graph), clearly disagree with the other PDFs. The mean values and, except for the final state, the CoVs as well, are much lesser (Table 5).

It is noticed that a similar discrepancy between testing and simulation also appears at some early stage of structural damage. Dymiotis et al. (1999) consider 52 RC specimens literally “tested not to failure” (another clear example of fuzziness in defining the damage state) under a relatively low axial load. On the assumption that the distribution is lognormal, the mean value of the drift is equal to 4.30 % and the CoV is 63.6 %. On the other hand, Lu and Gu (2004) carry out numerical simulation for RC columns with proper seismic detailing and axial load, at the performance level associated with the onset of cover crushing and residual cracks 1 mm wide at most. Much smaller parameter values result, namely the mean value is on the order of 1 % and CoV is on the order of 15 % with a normal distribution. Obviously, all of these do not suffice to draw general conclusions, but at least it stresses the importance of precise definition of the damage state, to minimise the fuzziness, and consistency between demand and capacity, both estimated either from testing or from simulation.

The code limits for masonry at the occupancy and life safety performance levels (Sect. 3.2.1) are marked along the abscissa axes in Fig. 10. According to the limit state design philosophy, such values should be the 0.05 percentile of the capacity distribution as regards the time-invariant serviceability, and the 0.005 percentile as regards the ultimate situation. The PDFs by Özcebe et al. (2012) clearly are too conservative. The PDFs with the fuzziness neglected for the third and fourth damage state by Colangelo (2013) are consistent with the code limits. In fact, the 0.05 percentile for repairable damage precisely is the drift value 0.279 % while it should be 0.3 %; the 0.005 percentile for irreparable damage precisely is the drift value 0.629 % while it should be 0.6 %. Such a very good agreement is lost with the PDFs with coupled randomness and fuzziness (shaded curves in Fig. 10). The capacity appears to increase because, it is repeated, the same whole uncertainty is now modelled in part in terms of fuzziness. Some preliminary analyses show that the fragility decreases to a noticeable extent once the fuzziness is accounted for (Colangelo 2013).

In this study, the PDF at repairable damage with the fuzziness taken into account is deemed to represent the infill capacity for the occupancy performance level as realistically as possible. Relevant parameters in Table 5 (third damage state by Colangelo 2013, final columns), and the demand parameters from the infilled frame analysis, are used to compute likely fuzzy-random fragility curves, to be compared with the code-compliant curves said in Sect. 3.2.1.

3.3 Estimation of fragility

The fragility specific to each storey is computed on the basis of the drift capacity, common to all storeys because they are similar, and individual demand. For the sake of brevity, the fragility of the frame as a whole is presented in this study. Computation of the storey and frame fragility is summarised in the next subsections.

3.3.1 Storey fragility

The aforementioned fuzzy–random model efficiently yields the storey fragility as an explicit function (Colangelo 2012, 2013). On the assumption that capacity and demand are lognormal and independent of each other, the fragility of the i -th storey is:

$$Pr_i = 1 + \frac{1}{\gamma^2} \sum_{h=1}^9 \alpha_h \Phi(\beta_h) \tag{8}$$

$\Phi()$ is the standard normal cumulative distribution function. As shown elsewhere (Colangelo 2012, 2013), α_h 's and β_h 's explicitly depend on: (i) the ratio of the mean values of capacity and demand to the i -th storey, μ_R/μ_S ; (ii) their CoVs, δ_R and δ_S ; and (iii) the fuzziness parameter γ . It is convenient to define an effective reliability index based on Eq. 8, that is, $\beta_i = -\Phi^{-1}(Pr_i)$. This makes it possible to compute the fuzzy–random fragility of a complex system similarly to its classical fragility with the fuzziness neglected, simply by treating the effective reliability indexes as the usual reliability indexes. Indeed, classical fragility may be seen as the special case where γ tends to zero in Eq. 8. Obviously, the case of capacity as a threshold value (code-compliant curve) may be treated as a special case as well, by putting $\delta_R = 0$ and $\mu_R = \text{threshold value}$.

Equation 8 gives the mean value of the degree of membership in the damage state considered as a fuzzy set; further probabilistic quantities have been formulated as well (Colangelo 2013). However, Eq. 8 and the concept of the effective reliability index suffice in order to compute the frame fragility as below.

3.3.2 Frame fragility

Consistent with the damage limitation verification (Eq. 6) to be satisfied at each and every storey, loss of occupancy of any storey is assumed to imply loss of occupancy of the whole building. Therefore, the frame is a serial system whose components are the storeys. It follows that the frame fragility is the union of the fragilities of the n storeys:

$$Pr = \Pr \left[\bigcup_{i=1}^n (z_i < -\beta_i) \right] \tag{9}$$

Equation 9 involves the effective reliability indexes β_i 's of all storeys and related standard normal random variables:

$$Z_i = \frac{\ln(R_i/S_i) - \mu_{\ln R_i} + \mu_{\ln S_i}}{\sqrt{\sigma_{\ln R_i}^2 + \sigma_{\ln S_i}^2}} \tag{10}$$

It is convenient to formulate Eq. 9 by intersection and matrix notation:

$$Pr = 1 - \Pr \left[\bigcap_{i=1}^n (z_i > -\beta_i) \right] = 1 - \Pr \left[\bigcap_{i=1}^n (z_i < \beta_i) \right] = 1 - \Phi_n(\boldsymbol{\beta}, \mathbf{C}) \tag{11}$$

$\Phi_n()$ is the n -variate standard normal cumulative distribution function. $\boldsymbol{\beta}$ is the vector collecting the effective reliability indexes. \mathbf{C} is the correlation matrix whose terms can be shown to have the following expression, provided that each capacity is uncorrelated with each demand:

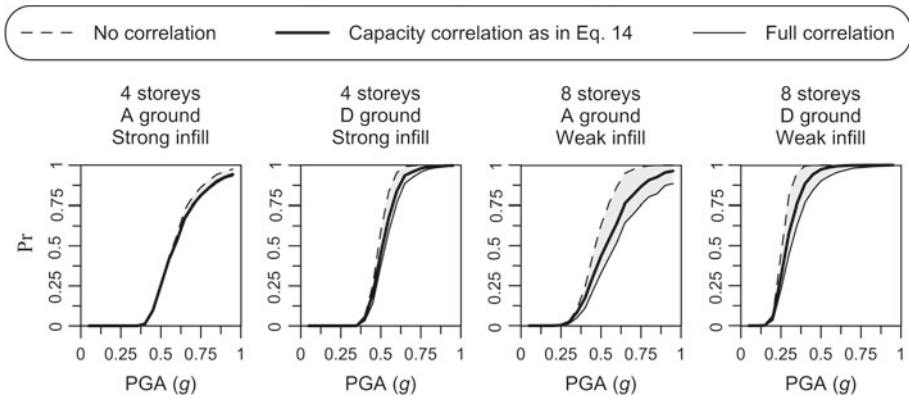


Fig. 11 Sensitivity to correlation between storeys (DCM frames)

$$c_{ij} = \frac{\sigma_{\ln R_i R_j} + \sigma_{\ln S_i S_j}}{\sqrt{(\sigma_{\ln R_i}^2 + \sigma_{\ln S_i}^2) (\sigma_{\ln R_j}^2 + \sigma_{\ln S_j}^2)}} \tag{12}$$

Elementary relationships give the log-correlation between the demands to the *i*-th and *j*-th storeys, or between their capacities as well:

$$\sigma_{\ln X_i X_j} = \ln \left(1 + \frac{\sigma_{X_i X_j}}{\mu_{X_i} \mu_{X_j}} \right) = \ln (1 + \rho_{X_i X_j} \delta_{X_i} \delta_{X_j}) \tag{13}$$

The correlation coefficients ρ between the demands are calculated at each PGA value as statistics on the drift values from the time-history analyses. As regards the correlation coefficients between the capacities, there is a lack of information. Clearly, the farther the storeys, the smaller the correlation, because of an increased likelihood of the use of infill materials from different supplies, and different aging condition because of varying temperature, humidity etc. In this study, the correlation coefficients between the capacities are assumed to be as follows:

$$\rho_{R_i R_j} = \begin{cases} 0.75 & i = j + 1 \\ 0.50 & i = j + 2 \\ 0.25 & i \geq j + 3 \end{cases} \tag{14}$$

The effect on the fragility curve is appraised by comparison with the results in the extreme cases of full correlation and no correlation. Then the fragility respectively becomes minimum and maximum, and Eq. 9 reduces as follows:

$$\begin{aligned} \Pr_{\min} &= \max_i [\Pr (z_i < -\beta_i)] \\ \Pr_{\max} &= 1 - \prod_{i=1}^n [1 - \Pr (z_i < -\beta_i)] \end{aligned} \tag{15}$$

A few results are shown (Fig. 11). The fragility curves according to Eq. 14 appear to be intermediate, as is obvious, and a little bit closer to the low bounds from full correlation.

As regards computation, the multi-normal integral implicit in Eq. 11 is estimated by the product of conditional marginal method (Yuan and Pandey 2006).

4 Fragility curves

The fragility curves according to the methodology above are illustrated in Figs. 12, 13, 14 and 15. The same curves appear in these figures, with the arrangement suitable for each aspect under consideration, that is: the kind of fragility estimation, the number of storeys, the ground type, and the ductility class. Two PGA values are emphasised as shaded thresholds in every graph. They are the design PGA for ultimate situation (0.25 g, light shade) and relevant PGA for occupancy (dark shade), taken equal to the design PGA for ultimate situation times the reduction factor in Eq. 6, which makes 0.125 g.

4.1 Kind of fragility estimation

The difference between the code-compliant curves (it is recalled, those from the bare frame analysis with capacity treated as a threshold value) and likely curves (those from the infilled frame analysis with capacity treated as a random variable and fuzziness in the damage state included) is best seen in Fig. 12. The fragility according to the code-compliant curves is substantially greater. Certainly, some overestimation is due to the capacity being treated as a threshold value lesser than the mean value of the distribution (Colangelo 2012). Using a threshold also causes the fragility curve to be steeper (Colangelo 2012), as it clearly appears in Fig. 12. Nonetheless, the code-compliant curves rise at a PGA comparable with the design PGA, whereas the fuzzy-random curves in most cases rise at a much greater PGA, which does not appear to be the effect of modelling the randomness of capacity (Colangelo 2012). Therefore, the effect of modelling the infills has to be admitted. Besides, the fragility in Fig. 12 depends on the kind of the infills, being minimum in the case of the strong (stiff)

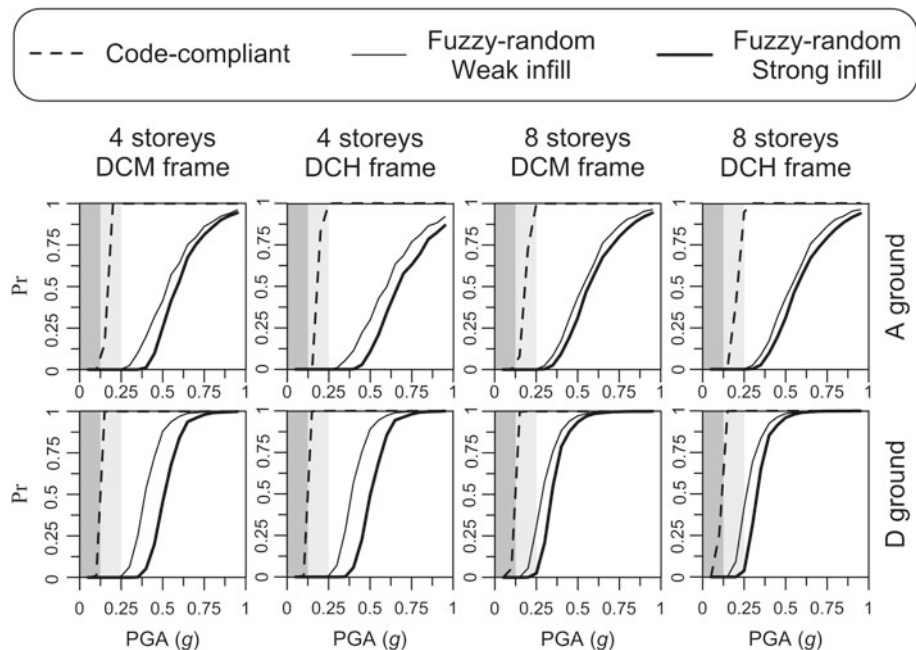


Fig. 12 Code-compliant fragility versus fuzzy-random fragility

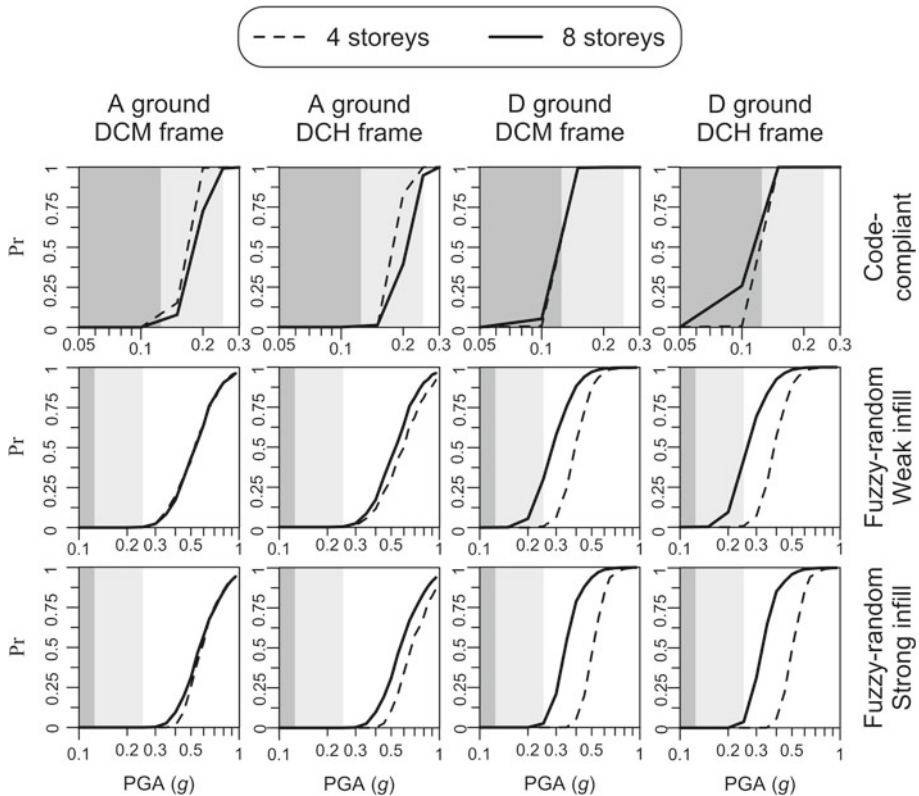


Fig. 13 Fragility of 4-storey frames versus fragility of 8-storey frames

infills. The code-compliant curves are on the safe side with respect to the fuzzy–random curves, as it should be due to simplification. However, the margin appears to be inconsistent in that relatively small for both the 8-storey frames on the type D ground (bottom right graphs).

4.2 Number of storeys

The effect of the number of storeys is best seen in Fig. 13. The code-compliant curves (top graphs) suggest different results depending on the ground type. On the type A ground (top left graphs) the fragility is greater in the case of the 4-storey frames, but on the type D ground (top right graphs) the fragility is almost the same, or greater only in the case of the 8-storey DCH frame under a low PGA. According to the fuzzy–random curves (middle and bottom graphs), on the type A ground (left graphs) the fragility is either similar or greater in the case of the 8-storey frames, which is contrary to the code-compliant curves; on the type D ground (right graphs) the fragility clearly and systematically is greater in the case of the 8-storey frames. All in all, the code-compliant curves misrepresent the effect of the number of storeys.

4.3 Ground type

The effect of the ground type is best seen in Fig. 14. All curves agree on fragility being greater on the type D ground. This reflects the (bare) frame design governed by the damage

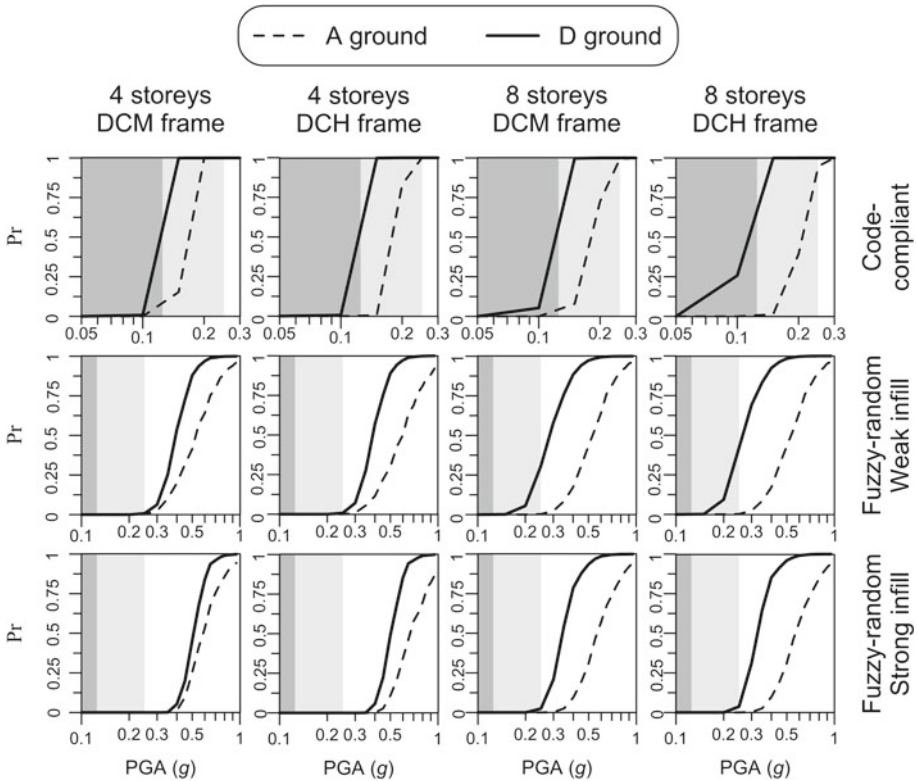


Fig. 14 Fragility on type A ground versus fragility on type D ground

limitation verification (Eq. 6) on the type D ground, as opposed to the condition about second order effects (Eq. 5) governing on the type A ground (Sect. 2.3). On the type A ground there is a margin in the damage limitation verification, thus performance is better than on the type D ground where any margin is missing. This remark applies to the frames analysed infilled as well (fuzzy–random curves, middle and bottom graphs in Fig. 14), despite the infills cause the base shear to increase on the type A ground only (see V_{base} in Tables 3 and 4 again). With regard to the type A ground, the margin in Eq. 6 of each 8-storey frame is greater than the margin of the corresponding 4-storey frame (consider how Δ_{max} is less than the limit 0.5 % in Table 3 as opposed to Table 4). Consistently, the fuzzy–random curves on the type A ground are farthest from the curves on the type D ground, where there is not any margin in Eq. 6, in the case of the 8-storey frames (Fig. 14, right graphs), while the curves get closer in the case of the 4-storey frames (left graphs), under a relatively low PGA especially. The code-compliant curves (top graphs) do not capture this aspect equally well, despite they are expected to do in that based on the analysis of bare frames like the damage limitation verification.

Since the frames on the type D ground with no margin meet the damage limitation verification, there is the opportunity to verify whether such a provision is effective against loss of occupancy. The code-compliant curves of the 4-storey frames on the type D ground (top left graphs in Fig. 14, solid line) precisely rise at the design PGA for occupancy (it is recalled that discrete fragility is computed at 0.10 and 0.15 g). Unexpectedly, the code-compliant curves of the 8-storey frames on the type D ground (top right graphs, solid line) rise at lower PGA, in

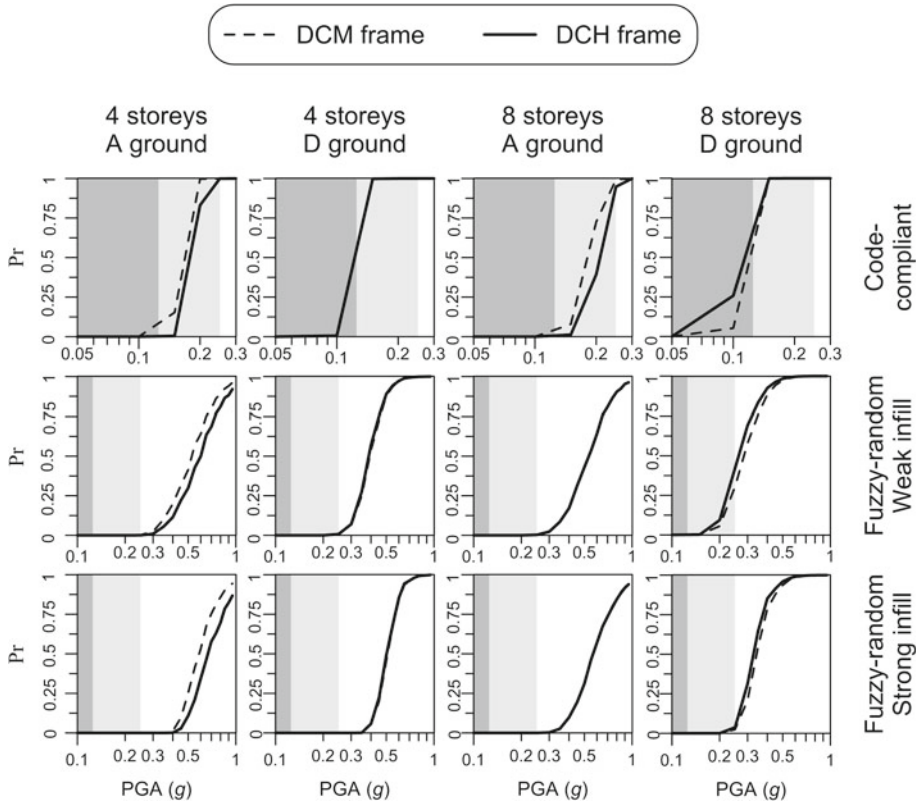


Fig. 15 Fragility of DCM frames versus fragility of DCH frames

the case of the DCH frame especially. Therefore, the damage limitation verification may not ensure the performance which the Eurocode 8 aims at. All the more so because randomness of the material properties, not considered herein, makes the fragility to increase at low PGA (Colangelo 2012). Fortunately, as one would say, there is the effect of the infills to outline a different situation. All the fuzzy–random curves (middle and bottom graphs, solid line) rise at a PGA greater than the design PGA for occupancy, and even greater than the design PGA for ultimate situation in the case of the 4-storey frames (left graphs). In confirmation of the positive effect of the infills, note that the fragility with weak infills is greater than the fragility with strong infills (compare each middle graph with the corresponding bottom graph), as already seen in Fig. 12. In the worst cases, those of the 8-storey frames with weak infills on the type D ground (middle right graphs in Fig. 14, solid line), loss of occupancy appears to be highly probable at the design PGA for ultimate situation.

4.4 Ductility class

The effect of the ductility class is best seen in Fig. 15. The ductility class seems to be of little consequence, so much so that a number of curves almost overlap. However, some correlation with the likely strength (Sect. 2.3) appears. As it is, the 4-storey DCH frames on the type A ground are a little stronger than the DCM frames (Fig. 3, leftmost graph) and their fragility is a little lesser (Fig. 15, leftmost graphs). On the other hand, the 8-storey DCH frames

on the type D ground are weaker than the DCM frames (Fig. 3, rightmost graph) and their fragility is a little greater (Fig. 15, rightmost graphs). All in all, the strength of the remaining frames is similar (Fig. 3, centre graphs) and their fragility is as well (Fig. 15, centre graphs). Finally, the 8-storey frames on the type D ground have the smallest surplus of likely strength compared with the design strength (Fig. 3, rightmost graph) and their fragility is the greatest (compare each rightmost graph in Fig. 15 with the graphs on the same row). This is rational because inelastic displacement and drift do depend on the strength, contrary to the equal displacement rule. Cyclic deterioration and damage are expected to be heavier with a lesser strength. However, this point would deserve further investigation.

5 Conclusion

The seismic performance in terms of drift-sensitive non-structural damage to masonry-infilled RC frames designed to Eurocode 8 is presented. The fragility against loss of occupancy is computed by numerical simulation with different degrees of complexity. First, the fragility curves fully complying with the code provisions are estimated on the basis of the bare frame analysis with capacity treated as a threshold value. Second, likely curves are estimated from the infilled frame analysis with capacity treated as a random variable and fuzziness in the damage state included.

Modelling the masonry infills, even partitions, is essential to capture likely drift and fragility. The code-compliant curves honestly are on the safe side with respect to the fuzzy-random curves, but their margin appears to be inconsistent among the frames under consideration. Moreover, the code-compliant curves are misleading about the effect of the number of storeys and they do not reflect the surplus in the damage limitation verification as well as the fuzzy-random curves do. Most importantly, there is one result suggesting that occupancy may be not ensured despite the damage limitation verification is satisfied. Such an inconsistency does not appear in the fuzzy-random curves. The ductility class of the frames under consideration is unimportant, but this result may be accidental in that due to the likely strength of the frames being similar. This point should be investigated further. Additional study is also necessary for different infills, because many types exist in Europe, and for possible effects of irregularity and torsion of the building, not considered herein.

Putting into practise, modelling the masonry infills would be advisable, as is obvious. Otherwise, the Eurocode 8 provisions about conventional damage limitation verification might be improved at least by distinguishing the drift limits depending on the design parameters. For instance, according to this study, the stronger the infill, the greater the limit, which is already implemented in the FEMA (2000) prestandard. Similarly, the greater the number of storeys, the smaller the limit. Future calibration can be based on the fuzzy-random approach with extensive numerical simulation. A weakness of this methodology is the present scarcity of statistical data to identify the capacity distribution coupled with the fuzziness parameter.

Acknowledgments This study was partly funded by the Italian Ministry of Education, University, and Research (MIUR) with Grant No. 2010MBJK5B_006.

References

- Augenti N, Parisi F (2010) Learning from construction failures due to the 2009 L'Aquila, Italy, earthquake. *J Perform Constr Facil* 24(6):536–555. doi:[10.1061/\(ASCE\)CF.1943-5509.0000122](https://doi.org/10.1061/(ASCE)CF.1943-5509.0000122)

- Bommer JJ, Magenes G, Hancock J, Penazzo P (2004) The influence of strong-motion duration on the seismic response of masonry structures. *Bull Earthq Eng* 2(1):1–26. doi:[10.1023/B:BEEE.0000038948.95616.bf](https://doi.org/10.1023/B:BEEE.0000038948.95616.bf)
- Braga F, Manfredi V, Masi A, Salvatori A, Vona M (2011) Performance of non-structural elements in RC buildings during the L'Aquila, 2009 earthquake. *Bull Earthq Eng* 9(1):307–324. doi:[10.1007/s10518-010-9205-7](https://doi.org/10.1007/s10518-010-9205-7)
- Calvi GM (1999) A displacement-based approach for vulnerability evaluation of classes of buildings. *J Earthq Eng* 3(3):411–438. doi:[10.1080/13632469909350353](https://doi.org/10.1080/13632469909350353)
- CEN (2002a) EN 1990 Eurocode: basis of structural design. European Committee for Standardization, Brussels
- CEN (2002b) EN 1991-1-1 Eurocode 1: actions on structures-Part 1–1: general actions. European Committee for Standardization, Brussels
- CEN (2004a) EN 1992 Eurocode 2: design of concrete structures. European Committee for Standardization, Brussels
- CEN (2004b) EN 1998-1 Eurocode 8: design of structures for earthquake resistance-Part 1: general rules, seismic actions and rules for buildings. European Committee for Standardization, Brussels
- CEN (2005) EN 1998-3 Eurocode 8: design of structures for earthquake resistance-Part 3: assessment and retrofitting of buildings. European Committee for Standardization, Brussels
- CM 617 (2009) Istruzioni per l'applicazione delle nuove norme tecniche per le costruzioni. Ministero delle Infrastrutture e dei Trasporti, Rome (in Italian)
- Colangelo F (2003) Experimental evaluation of member-by-member models and damage indices for infilled frames. *J Earthq Eng* 7(1):25–50. doi:[10.1142/S1363246903000821](https://doi.org/10.1142/S1363246903000821)
- Colangelo F (2005) Pseudo-dynamic seismic response of reinforced concrete frames infilled with non-structural brick masonry. *Earthq Eng Struct Dyn* 34(10):1219–1241. doi:[10.1002/eqe.477](https://doi.org/10.1002/eqe.477)
- Colangelo F (2012) A simple model to include fuzziness in the seismic fragility curve and relevant effect compared with randomness. *Earthq Eng Struct Dyn* 41(5):969–986. doi:[10.1002/eqe.1169](https://doi.org/10.1002/eqe.1169)
- Colangelo F (2013) Probabilistic characterisation of an analytical fuzzy-random model for seismic fragility computation. *Struct Safety* 40:68–77. doi:[10.1016/j.strusafe.2012.09.008](https://doi.org/10.1016/j.strusafe.2012.09.008)
- Colangelo F, Stornelli P (2008) Seismic damage of nonstructural masonry infills: statistical characterization by interstory drift and stiffness decrease. In: Proceedings of the 8th US national conference on earthquake engineering, paper 821
- DM 14/1/2008(2008) Norme tecniche per le costruzioni. Ministero delle Infrastrutture e dei Trasporti, Rome (in Italian)
- Draper NR, Smith H (1998) Applied regression analysis, 3rd edn. Wiley, New York
- Dymiotis C, Kappos AJ, Chryssanthopoulos MK (1999) Seismic reliability of RC frames with uncertain drift and member capacity. *J Struct Eng* 125(9):1038–1047. doi:[10.1061/\(ASCE\)0733-9445\(1999\)125:9\(1038\)](https://doi.org/10.1061/(ASCE)0733-9445(1999)125:9(1038))
- Fardis MN, Papailia A, Tsionis G (2012) Seismic fragility of RC framed and wall-frame buildings designed to the EN-Eurocodes. *Bull Earthq Eng* 10(6):1767–1793. doi:[10.1007/s10518-012-9379-2](https://doi.org/10.1007/s10518-012-9379-2)
- FEMA (2000) Prestandard and commentary for the seismic rehabilitation of buildings. Report FEMA 356, Federal Emergency Management Agency, Washington
- FEMA (2003) Multi-hazard loss estimation methodology-Earthquake model HAZUS-MH MR4 technical manual. Federal Emergency Management Agency, Washington
- Ghobarah A (2004) On drift limits associated with different damage levels. In: Fajfar P, Krawinkler H (eds) Performance-based seismic design concepts and implementation. PEER report 2004/05, Pacific Earthquake Engineering Research Center, Berkeley, pp 321–332
- Gu X, Lu Y (2005) A fuzzy-random analysis model for seismic performance of framed structures incorporating structural and non-structural damage. *Earthq Eng Struct Dyn* 34(10):1305–1321. doi:[10.1002/eqe.481](https://doi.org/10.1002/eqe.481)
- Hill M, Rossetto T (2008) Comparison of building damage scales and damage descriptions for use in earthquake loss modelling in Europe. *Bull Earthq Eng* 6(2):335–365. doi:[10.1007/s10518-007-9057-y](https://doi.org/10.1007/s10518-007-9057-y)
- Iervolino I, Manfredi G, Cosenza E (2006) Ground motion duration effects on nonlinear seismic response. *Earthq Eng Struct Dyn* 35(1):21–38. doi:[10.1002/eqe.529](https://doi.org/10.1002/eqe.529)
- Litton RW (1975) A contribution to the analysis of concrete structures under cyclic loading. PhD thesis, Department of Civil Engineering, University of California, Berkeley
- Lu Y, Gu XM (2004) Probability analysis of RC member deformation limits for different performance levels and reliability of their deterministic calculations. *Struct Safety* 26(4):367–389. doi:[10.1016/j.strusafe.2004.01.001](https://doi.org/10.1016/j.strusafe.2004.01.001)
- Masi A (2003) Seismic vulnerability assessment of gravity load resisted R/C frames. *Bull Earthq Eng* 1(3):371–395. doi:[10.1023/B:BEEE.0000021426.31223.60](https://doi.org/10.1023/B:BEEE.0000021426.31223.60)
- Mondkar DP, Powell GH (1975a) Static and dynamic analysis of nonlinear structures. Report UCB/EERC-75/10, Earthquake Engineering Research Center, University of California, Berkeley
- Mondkar DP, Powell GH (1975b) ANSR-I: general purpose program for analysis of nonlinear structural response. Report UCB/EERC-75/37, Earthquake Engineering Research Center, University of California, Berkeley

- Mosalam KM, Ayala G, White RN, Roth C (1997) Seismic fragility of LRC frames with and without masonry infill walls. *J Earthq Eng* 1(4):693–720. doi:[10.1142/S1363246997000271](https://doi.org/10.1142/S1363246997000271)
- Ólafsson S, Sigbjörnsson R (2011) Digital filters for simulation of seismic ground motion and structural response. *J Earthq Eng* 15(8):1212–1237. doi:[10.1080/13632469.2011.565862](https://doi.org/10.1080/13632469.2011.565862)
- Otani A (1974) Inelastic analysis of reinforced concrete frame structures. *J Struct Div* 100(ST7):1433–1449
- Özcebe S, Crowley H, Bal IE (2012) Distinction between no and slight damage states for existing RC buildings using a displacement-based approach. In: Proceedings of the 15th world conference on earthquake engineering, paper 5126.
- Panagiotakos TB, Fardis MN (1997) Infill macromodel developed at the University of Patras. In: Fardis MN (ed) Experimental and numerical investigations on the seismic response of RC infilled frames and recommendations for code provisions. Report 6 of PREC8/ECOEST projects, Laboratório Nacional de Engenharia Civil, Lisbon
- Press WH, Teukolsky SA, Vetterling WT, Flannery BP (2007) Numerical recipes: the art of scientific computing, 3rd edn. Cambridge University Press, Cambridge
- Ricci P, De Risi MT, Verderame GM, Manfredi G (2012) Influence of infill presence and design typology on seismic performance of RC buildings: fragility analysis and evaluation of code provisions at damage limitation limit state. In: Proceedings of the 15th world conference on earthquake engineering, paper 5836
- Rivera JA, Petrini L (2011) On the design and seismic response of RC frame buildings designed with Eurocode 8. *Bull Earthq Eng* 9(5):1593–1616. doi:[10.1007/s10518-011-9290-2](https://doi.org/10.1007/s10518-011-9290-2)
- Rossetto T, Elnashai A (2003) Derivation of vulnerability functions for European-type RC structures based on observational data. *Eng Struct* 25(10):1241–1263. doi:[10.1016/S0141-0296\(03\)00060-9](https://doi.org/10.1016/S0141-0296(03)00060-9)
- Rozman M, Fajfar P (2009) Seismic response of a RC frame building designed according to old and modern practices. *Bull Earthq Eng* 7(3):779–799. doi:[10.1007/s10518-009-9119-4](https://doi.org/10.1007/s10518-009-9119-4)
- Saaty TL (2008) Relative measurement and its generalization in decision making; why pairwise comparisons are central in mathematics for the measurement of intangible factors; the analytic hierarchy/network process. *Rev R Acad Cien Serie A Mat* 102(2):251–318. doi:[10.1007/BF03191825](https://doi.org/10.1007/BF03191825)
- Shinozuka M, Deodatis G (1991) Simulation of stochastic processes by spectral representation. *Appl Mech Rev* 44(4):191–204. doi:[10.1115/1.3119501](https://doi.org/10.1115/1.3119501)
- Soong TT (2004) Fundamentals of probability and statistics for engineers. Wiley, Chichester
- Taghavi S, Miranda E (2003) Response assessment of nonstructural building elements. PEER report 2003/05, Pacific Earthquake Engineering Research Center, Berkeley.
- Takeda T, Sozen MA, Nielsen NN (1970) Reinforced concrete response to simulated earthquakes. *J Struct Div* 96(ST12):2557–2573
- Vanmarcke EH (1976) Structural response to earthquakes. In: Lomnitz C, Rosenblueth E (eds) Seismic risk and engineering decisions. Elsevier, Amsterdam, pp 287–337
- Vanmarcke EH, Cornell CA, Gasparini DA, Hou SN (1976) Simulation of earthquake ground motions. Department of Civil Engineering, Massachusetts Institute of Technology, Cambridge
- Yuan X-X, Pandey MD (2006) Analysis of approximations for multinormal integration in system reliability computation. *Struct Safety* 28(4):361–377. doi:[10.1016/j.strusafe.2005.10.002](https://doi.org/10.1016/j.strusafe.2005.10.002)
- Zadeh LA (1968) Probability measures of fuzzy events. *J Math Anal Appl* 23(2):421–427. doi:[10.1016/0022-247X\(68\)90078-4](https://doi.org/10.1016/0022-247X(68)90078-4)
- Zovkic J, Sigmund V, Guljas I (2013) Cyclic testing of single bay reinforced concrete frames with various types of masonry infill. *Earthq Eng Struct Dyn* 42(8):1131–1149. doi:[10.1002/eqe.2263](https://doi.org/10.1002/eqe.2263)